OXFORD
SOT | Society of Toxicology
www.toxsci.oxfordjournals.org

TOXICOLOGICAL SCIENCES, 141(2), 2014, 409–422

doi: 10.1093/toxsci/kfu144
Advance Access Publication Date: July 28, 2014

Repeated Gestational Exposure of Mice to Chlorpyrifos Oxon Is Associated with Paraoxonase 1 (PON1) Modulated Effects in Maternal and Fetal Tissues

Toby B. Cole*,†,‡,§,1, Wan-Fen Li*,1, Aila L. Co*,‡, Ariel M. Hay*,‡, James W. MacDonald†,¶, Theo K. Bammler†,¶, Federico M. Farin†,¶, Lucio G. Costa†,‖, and Clement E. Furlong*,‡,2

*Department of Medicine, Division of Medical Genetics, †Department of Environmental and Occupational Health Sciences, ‡Department of Genome Sciences, §Center on Human Development and Disability, ¶Center for Ecogenetics and Environmental Health, University of Washington, Seattle, Washington 98195 and ‖Department of Neuroscience, University of Parma, Parma, Italy

[1]These authors contributed equally to this work.
[2]To whom correspondence should be addressed. Fax: +1 206-543-3050; E-mail: clem@u.washington.edu.

ABSTRACT

Chlorpyrifos oxon (CPO), the toxic metabolite of the organophosphorus (OP) insecticide chlorpyrifos, causes developmental neurotoxicity in humans and rodents. CPO is hydrolyzed by paraoxonase-1 (PON1), with protection determined by PON1 levels and the human Q192R polymorphism. To examine how the Q192R polymorphism influences fetal toxicity associated with gestational CPO exposure, we measured enzyme inhibition and fetal-brain gene expression in wild-type (*PON1*$^{+/+}$), *PON1*-knockout (*PON1*$^{-/-}$), and *tgHuPON1*$_{R192}$ and *tgHuPON1*$_{Q192}$ transgenic mice. Pregnant mice exposed dermally to 0, 0.50, 0.75, or 0.85 mg/kg/d CPO from gestational day (GD) 6 through 17 were sacrificed on GD18. Biomarkers of CPO exposure inhibited in maternal tissues included brain acetylcholinesterase (AChE), red blood cell acylpeptide hydrolase (APH), and plasma butyrylcholinesterase (BChE) and carboxylesterase (CES). Fetal plasma BChE was inhibited in *PON1*$^{-/-}$ and *tgHuPON1*$_{Q192}$, but not *PON1*$^{+/+}$ or *tgHuPON1*$_{R192}$ mice. Fetal brain AChE and plasma CES were inhibited in *PON1*$^{-/-}$ mice, but not in other genotypes. Weighted gene co-expression network analysis identified five gene modules based on clustering of the correlations among their fetal-brain expression values, allowing for correlation of module membership with the phenotypic data on enzyme inhibition. One module that correlated highly with maternal brain AChE activity had a large representation of homeobox genes. Gene set enrichment analysis revealed multiple gene sets affected by gestational CPO exposure in *tgHuPON1*$_{Q192}$ but not *tgHuPON1*$_{R192}$ mice, including gene sets involved in protein export, lipid metabolism, and neurotransmission. These data indicate that maternal PON1 status modulates the effects of repeated gestational CPO exposure on fetal-brain gene expression and on inhibition of both maternal and fetal biomarker enzymes.

Key words: Chlorpyrifos oxon; microarrays; neurotoxicity; organophosphorus insecticides; paraoxonase-1; transgenic mice

The organophosphorus (OP) compound chlorpyrifos (CPS) is one of the most extensively used insecticides worldwide. The residential use of CPS in the United States has been eliminated since 2000 due to its potential as a developmental neurotoxicant (USEPA, 2006). However, CPS is still widely used in agriculture, with about 10 million pounds applied to a large variety of crops, and poses a risk for exposure of children through take-home contamination in agricultural households or via the dietary pathway in urban areas. The classic mechanism of CPS toxicity is through inhibition of acetylcholinesterase (AChE) by

its active metabolite chlorpyrifos oxon (CPO) although many other serine hydrolases are also inhibited by CPO. The highly toxic CPO is also formed in the environment through reaction with oxidizing agents and has been detected in foliage (Yuknavage *et al.*, 1997), air samples (Armstrong *et al.*, 2013a,b), and vegetables harvested from greenhouses (Vidal *et al.*, 1998). CPO represented 2–14% of total CPS exposure in air samples (Armstrong *et al.*, 2013b) and CPO residues in green beans and tomatoes were reported to be as high as 0.14–0.21 mg/kg (Vidal *et al.*, 1998).

Evidence from epidemiologic studies has suggested that OP exposure during pregnancy has adverse effects on birth outcomes and neurodevelopment of children. Prenatal exposure to OP pesticides was negatively associated with child neurobehavioral performance including abnormal reflexes in infants (Engel *et al.*, 2007; Young *et al.*, 2005), mental and psychomotor development delay in toddlers (Eskenazi *et al.*, 2007; Rauh *et al.*, 2006), as well as lower IQ and poorer cognitive development in school children (Bouchard *et al.*, 2011; Engel *et al.*, 2011). Studies using cell cultures and animal models have also indicated that CPS can interfere with normal brain development. CPS and CPO were shown to induce cytotoxicity in both neuronal and glial cells (Monnet-Tschudi *et al.*, 2000), inhibit DNA synthesis in rat brain (Dam *et al.*, 1998) and in cultures of neurons, glia, and astrocytes (Guizzetti *et al.*, 2005; Qiao *et al.*, 2001). At the morphological level, CPS and CPO also decreased total axonal length (Howard *et al.*, 2005). Furthermore, treatment with CPS or CPO altered the expression and function of transcription factors such as AP-1, Sp1, and CREB, which mediate cell replication and differentiation (Crumpton *et al.*, 2000; Schuh *et al.*, 2002).

These *in vitro* and *in vivo* neurotoxic effects were found at doses that are below the threshold of inducing significant AChE inhibition, indicating that the action of CPS/CPO on developing brain may be through different pathways than inhibition of AChE enzymatic activity. It has also been suggested that CPO, with a much higher potency than CPS, may act directly on the morphogenic capability of AChE and on targets such as cell signaling molecules or cytoskeleton proteins (Flaskos, 2012). A major detoxification pathway of CPO is through hydrolysis by paraoxonase 1 (PON1) as shown by dramatically increased sensitivity to CPO in *PON1*-knockout mice (Shih *et al.*, 1998). The PON1 Q192R polymorphism determines catalytic efficiency of the enzyme for hydrolyzing CPO, with the $PON1_{R192}$ alloform providing greater protection than the $PON1_{Q192}$ alloform against CPO toxicity (Cole *et al.*, 2005; Li *et al.*, 2000). Epidemiologic studies have demonstrated that both maternal PON1 activity level and the status of her Q192R polymorphism play a role in modulating the association between OP exposure and child neurodevelopment. Maternal PON1 activity level was found to modify the adverse effects of OP exposure on head circumstance of newborns (Berkowitz *et al.*, 2004) and on mental and psychomotor development assessed at 2 years of age (Eskenazi *et al.*, 2010), whereas the OP-related decrease in perceptual reasoning was found only in children whose mothers were of QQ genotype (Engel *et al.*, 2011). However, most prenatal OP exposure studies in animals did not address the role of PON1 in OP-related developmental toxicity.

Previously, a toxicogenomic approach has been used to examine the effects of CPS/CPO on gene expression profiles by gestational CPS exposure in mice (Moreira *et al.*, 2010), by postnatal CPS exposure in neonatal rats (Betancourt *et al.*, 2006; Ray *et al.*, 2010; Slotkin and Seidler, 2007), by postnatal CPO exposure in neonatal mice (Cole *et al.*, 2011), and by CPS exposure in adult rats (Stapleton and Chan, 2009) or PC12 cells (Slotkin and Seidler, 2009; Slotkin *et al.*, 2008). To understand the neurotoxicity of CPO in fetuses following chronic *in utero* exposure and to examine the importance of the maternal PON1 Q192R polymorphism in protecting fetuses against CPO, we used genome-wide microarrays to measure gene expression changes associated with repeated gestational CPO exposure (GD6 to GD17) in fetal brains of wild type, *PON1*-knockout, and humanized *PON1* transgenic mice that carry either the human R_{192} or the Q_{192} allele over a *PON1*-knockout background.

MATERIALS AND METHODS

Animals. *PON1* knockout ($PON1^{-/-}$) mice (Shih *et al.*, 1998) and mice expressing either the human $PON1_{R192}$ or $PON1_{Q192}$ transgene ($tgHuPON1_{R192}$ or $tgHuPON1_{Q192}$) in place of endogenous mouse *PON1* (Cole *et al.*, 2003, 2005) were provided by Dr. Diana M. Shih, Dr. Aaron Tward, and Dr. Aldons J. Lusis (UCLA, Los Angeles, CA). Mice with at least one copy of the transgene were crossed with same-genotype animals to produce both $PON1^{-/-}$ mice and transgenic mice ($tgHuPON1_{R192}$ or $tgHuPON1_{Q192}$) in the same litter. Wild-type ($PON1^{+/+}$) mice were bred from the same congenic B6.129 strain background. Presence of $PON1_{Q192}$ or $PON1_{R192}$ enzyme activity in heparinized saphenous-vein plasma was detected by measuring the rate of hydrolysis of the alloform-neutral substrate, diazoxon, which is alloform-neutral at 0.5 M NaCl (Richter and Furlong, 1999) and has no background activity in $PON1^{-/-}$ mice (Cole *et al.*, 2003). Polymerase chain reaction (PCR) based genotyping was used to determine the presence of the transgenes.

Mice were housed in specific pathogen-free facilities with a 12-h dark-light cycle and unlimited access to food and water. The animal use protocols used were approved by the Institutional Animal Care and Use Committee at the University of Washington. All animal experiments were carried out in accordance with the National Research Council Guide for the Care and Use of Laboratory Animals, as adopted by the National Institutes of Health.

Chemicals. Chlorpyrifos oxon (CAS 5598-15-2; 98% purity) and diazoxon (CAS 962-58-3; 99% purity) were purchased from Chem Service (West Chester, PA). Acetylthiocholine iodide, butyrylthiochoine iodide, 5,5′-dithio-bis-nitrobenzoic acid, and *p*-nitrophenyl valerate were from Sigma-Aldrich (St Louis, MO). N-Acetyl-L-alanyl-*p*-nitroanilide was purchased from BACHEM (Torrance, CA). All other analytical grade chemicals were obtained from commercially available sources.

Exposure of mice to chlorpyrifos oxon (CPO). Timed matings of female $PON1^{+/+}$, $PON1^{-/-}$, and humanized transgenic mice ($tgHuPON1_{Q192}$ and $tgHuPON1_{R192}$) with males of the same genotype were used to generate pregnant females. The day the copulatory plug was visible was designated as gestational day (GD) 0. The dose of CPO exposure was determined based on the initial body weight of the dam at GD0. Body weights of all mice were measured daily just prior to dosing. Potentially pregnant mice were exposed dermally (1 μl/g body weight) to CPO (0, 0.50, 0.75, or 0.85 mg/kg/d) daily from GD6 to GD17. An 8.5 mg/ml stock solution of CPO dissolved in acetone was used to make serial dilutions for exposures. CPO was applied dermally to a shaved portion of the upper back and neck, using a Gilson P200 pipette, then the CPO was allowed to air-dry for 15 s, and the mouse was retained on the wire cage-top for 5 min before returning the mouse to its cage. Control mice received vehicle (acetone, > 99.9%) alone.

On GD18, 24 hr following the last exposure on GD17, pregnant mice were sacrificed by CO_2 asphyxiation, fetuses were staged (Theiler, 1989) and weighed, and maternal and fetal tissues were dissected for measurements of enzyme activity and gene expression. The experiments were conducted with two separate cohorts consisting of a total of 26 *PON1*$^{-/-}$ dams, 17 *PON1*$^{+/+}$ dams, 19 *tgHuPON1*$_{Q192}$ dams, and 20 *tgHuPON1*$_{R192}$ dams. Table 1 shows the pregnancy outcomes for each of the 12 genotype and treatment groups. Only dams with fetuses at Theiler Stage 26 were used for subsequent analysis. Maternal tissues collected included trunk blood, brain, liver, and diaphragm. Fetal tissues collected included trunk blood, brain, and liver. Trunk blood was collected into Vacutainer lithium-heparin tubes, followed by centrifugation to separate plasma from the erythrocytes, and stored at −80°C. Blood from fetuses of the same dam were combined into one tube prior to centrifugation. Brains from half of the fetuses of each dam were frozen on dry ice and stored at −80°C, and brains from the remaining fetuses were immersed in RNAlater solution (Ambion, Austin TX) for subsequent RNA extraction. Other tissues were frozen immediately on dry ice and stored at −80°C until analysis.

Sample preparation. Red blood cells (RBC) were frozen and thawed on dry ice twice to lyse cells and further diluted 1:80 with 100 mM Tris-HCl, pH 7.5 for assays. Frozen brains were thawed and homogenized in 0.1 M sodium phosphate buffer, pH 8 (6 vol v/w for maternal brains and 1 vol v/w for pooled fetal brains) using a handheld homogenizer (Tissue-Tearor, Cole-Parmer, IL). The crude homogenates were further diluted to 5 mg/ml (maternal samples) or 50 mg/ml (fetal samples) for assay. Frozen livers were homogenized using a Polytron homogenizer (Brinkmann Instruments, Westbury, NY) in 10 mM Tris-HCl, pH 7.5 and 0.25 M sucrose, and then centrifuged at 10,000 × g for 10 min at 4°C. Supernatants were centrifuged again at 15,000 × g for 20 min at 4°C to remove mitochondria. Microsomes were subsequently spun down at 110,000 × g for 30 min at 4°C using an ultracentrifuge (TL-100, Beckman Coulter Inc). Microsomal pellets were resuspended in 20 mM Tris-HCl, pH 7.5, 0.25 M sucrose, and 0.1 mM $CaCl_2$ and adjusted to a concentration of 5 mg protein/ml for assays. Protein concentration was determined by the Bradford method using a commercial assay kit (Coomassie Plus Assay Kit, Thermo Scientific Inc).

Enzyme activity assays. All the assays were carried out in triplicate using a SpectraMax Plus microtiter plate reader (Molecular Devices) with 96-well plates. Activities of chlorpyrifos-oxonase (CPOase), butyrylcholinesterase (BChE), and carboxylesterase (CES) were measured in maternal and fetal plasma. AChE activity was measured in maternal and fetal brains. Plasma as well as liver CPOase activities were measured as described previously (Furlong *et al.*, 1989). Plasma BChE and brain AChE activities were measured as described (Cole *et al.*, 2005) using butyrylthiocholine and acetylthiocholine as substrates, respectively. The initial rates of 5-thio-2-nitrobenzoate formed during the assay were monitored continuously at 412 nm for 4 min (plasma BChE) or 10 min (brain AChE) at room temperature. Plasma CES activity was measured as the rate of hydrolysis of *p*-nitrophenyl valerate, with the formation of *p*-nitrophenol monitored at 405 nm for 4 min at room temperature. Acylpeptide hydrolase (APH) activity of RBC was measured with a colorimetric method (Quistad *et al.*, 2005) using N-acetyl-L-alanyl-*p*-nitroanilide (Ac-Ala-pNA) as substrate. Twenty microliters of diluted (1:80) lysed RBC were added into individual wells containing 100 μl of 1.5 mg/ml Ac-Ala-pNA in 100 mM Tris-HCl, pH 7.5. Absorbance from liberated *p*-nitroaniline was continuously monitored at 405 nm for 4 min at 37°C.

For all assays, initial linear rates of product formation (mOD/min) for each enzyme were pathlength-corrected and converted to Units per ml (U/ml) or Units per gram (U/g) wet tissue using the respective extinction coefficients: 5-thio-2-nitrobenzoate, 13.6mM^{-1} cm^{-1}; *p*-nitrophenol, 18mM^{-1} cm^{-1}. Statistical differences in enzyme activities between treatment groups and genotypes were determined using Student's *t*-test.

RNA extraction, labeling, and microarray hybridization. Fetal brains were incubated in RNAlater for at least 12 h at 4°C, then stored at −80°C. Total RNA was isolated using TRIZOL Reagent and the QIAamp Tissue Kit from QIAGEN Inc, according to the manufacturer's established protocols. The quality of the total RNA was evaluated using an Agilent 2100 Bioanalyzer. There were a total of 264 fetal brain RNA samples representing 80 dams. RNA extracted from all samples had high integrity (RNA integrity number > 8), adequate RNA quantity, and A_{260}:A_{280} and A_{260}:A_{230} ratios of 1.8–2.1. A NanoDrop spectrophotometer (Thermo Scientific, Wilmington, DE) was used to determine these ratios and RNA concentrations were based on A_{260} measurements.

Affymetrix GeneChip Whole Transcript Sense Target Labeling and Hybridization. Microarray analysis was performed using the fetuses of five dams per experimental group. The dams used for fetal-brain microarray analysis were selected using a random-number generator, after first eliminating dams with brain AChE activities > 1.5 SD compared to the mean for their treatment group. RNA samples isolated from individual fetal brains from each dam were combined, then labeled and hybridized to Affymetrix Mouse Gene 1.0 ST microarrays. Microarray data quality control was assessed by Principal Components Analysis (PCA, not shown), plotting normalized unscaled standard errors (NUSE) and relative log-scale expression (RLE) values (Supplementary figs. 1A and B). In both NUSE and RLE plots, there were a few arrays that were slight outliers. These arrays were down-weighted in the analysis of variance (ANOVA) model to reduce their impact. An alternative would have been to remove these arrays from the analysis, but as it is difficult to decide on a cutoff for removal, and because doing so would lower the degrees of freedom and decrease the power to detect differences, we used a weighted ANOVA. Supplementary figure 1C shows MA plots comparing the log average of the expression data (horizontal axis; A) to the log difference between a given sample and the median of all samples (vertical axis; M) for each of the 60 array pools. Values were clustered tightly in an oval along the horizontal axis at zero, as would be expected from an ideal data set. In addition, all Affymetrix microarray data passed the manufacturer's QC metrics.

For MIAME compliance (Brazma *et al.*, 2001) raw data, final processed data, sample and array annotation, and experimental design have been submitted to the NCBI Gene Expression Omnibus (GEO) upon acceptance of the manuscript, and will be available at http://www.ncbi.nlm.nih.gov/geo/query/acc.cgi?acc=GSE58103 (release date: 1 January 2015).

Microarray data analysis: Individual gene analysis. Array data were summarized at the transcript level using a robust multi-array average (RMA) (Irizarry *et al.*, 2003), followed by fitting a weighted ANOVA model to the data, and comparisons between sample types by fitting empirical Bayes adjusted contrasts. By fitting a weighted ANOVA, we incorporated weights into the model, which allowed us to down-weight arrays that appear to be dis-

TABLE 1. Effects of Gestational Exposure to Chlorpyrifos Oxon (from Gestational Day 6 to 17) on Dams and Fetuses

Maternal data

	Body wt gain (%)				Adjusted body wt gain (%)				No. of implants per litter			
CPO dose (mg/kg/d)	WT	KO	R192	Q192	WT	KO	R192	Q192	WT	KO	R192	Q192
0	66.9 (6.2)	69.0 (7.1)	57.2 (3.5)	51.1 (5.5)	32.8 (3.7)	31.7 (4.0)	31.1 (1.7)	17.3 (3.3)	8.3 (0.9)	8.9 (0.4)	7.7 (0.8)	8.5 (0.9)
0.5	–	68.7 (6.3)	–	–	–	29.9 (4.0)	–	–	–	8.5 (2.7)	–	–
0.75	64.7 (7.4)	**48.5* (3.4)**	60.3 (2.5)	47.8 (4.4)	30.4 (5.4)	**20.1* (2.3)**	26.9 (1.5)	19.7 (4.4)	9.8 (0.6)	8.4 (0.8)	8.6 (3.2)	7.8 (0.3)
0.85	78.1 (5.9)	–	58.0 (8.6)	54.5 (6.1)	37.2 (3.7)	–	27.4 (2.6)	19.6 (3.8)	9.2 (0.4)	–	8.4 (1.3)	8.4 (0.7)

Fetal data

	Average fetal body wt (g)				No. of resorption per implant				No. of malformation per live fetus			
CPO dose (mg/kg/d)	WT	KO	R192	Q192	WT	KO	R192	Q192	WT	KO	R192	Q192
0	1.024 (0.045)	1.043 (0.035)	1.158 (0.026)	1.143 (0.028)	0.121 (0.044)	0.120 (0.066)	0.369 (0.078)	0.084 (0.039)	0.058 (0.042)	0.038 (0.024)	0.000 (0.000)	0.000 (0.000)
0.5	–	1.135 (0.020)	–	–	–	0.045 (0.024)	–	–	–	0.022 (0.015)	–	–
0.75	1.059 (0.013)	**0.918* (0.021)**	1.150 (0.029)	1.053 (0.032)	0.200 (0.024)	0.133 (0.034)	0.258 (0.046)	0.213 (0.058)	0.136 (0.088)	0.056 (0.028)	0.038 (0.025)	0.028 (0.028)
0.85	1.091 (0.026)	–	1.145 (0.021)	1.079 (0.032)	0.058 (0.042)	–	0.289 (0.077)	0.062 (0.033)	0.052 (0.035)	–	0.159 (0.141)	0.029 (0.029)

Notes. Data are presented as mean (SE).
Maternal body wt gain (%) = (maternal body wt at GD18–maternal body wt at GD0)/body wt at GD0.
Adjusted maternal body wt gain (%) = (maternal body wt at GD18–maternal body wt at GD0–litter wt)/body wt at GD0.
*$p < 0.05$ as compared with vehicle controls using Student's *t*-test. All the significant values are in bold.

similar to other arrays of the same type, and increase power of the data set (Ritchie *et al.*, 2006; Smyth, 2004). Supplementary table 1 lists the comparisons made, and the number of probesets selected at an unadjusted p value of 0.05 and an absolute fold change > 1.5.

WGCNA. As an alternative way to analyze these data, we used weighted gene co-expression network analysis (WGCNA), which uses the correlations between expression values to infer gene networks (Langfelder and Horvath, 2008). To subset the data, we removed all probesets with a standard deviation < 0.2, which resulted in 1598 probesets. Since there are multiple probesets per gene, and the duplicated probesets generally convey the same information, we further removed any duplicates, resulting in 719 genes. Finally, we subset the samples to just those samples that were treated with 0.75 mg/kg/d CPO. By-gene correlations were then computed, and gene "modules" were detected by clustering the correlation data. Figure 1A shows the clustering dendrogram. Gene clusters were then correlated with phenotypic data (maternal and fetal CPOase, brain AChE, plasma BChE, and plasma CES). Heat maps (Fig. 1B) were generated showing the correlation and correlation p value between each cluster and phenotypic measure. To more closely examine the genes in a given gene module with respect to a given phenotype, module membership, which infers the importance of a gene to the module, was plotted on the horizontal axis, and gene significance, which measures the correlation between a given gene and a phenotypic measure, was plotted on the vertical axis (Fig. 1C).

Gene set enrichment analysis. Gene set enrichment analysis (GSEA) aims to identify sets of genes that appear to be up- or downregulated. The gene sets that we used for this analysis were from the Broad Institute. The romer function from the Bioconductor limma package (R version 2.15.1) was used to perform GSEA. After completing GSEA, heat maps and data tables were generated for gene sets that had p values < 0.05.

Quantitative real-time PCR analysis. Thirty genes were chosen for validation by quantitative PCR (qPCR) based on either p value and fold change from the univariate comparisons, membership in specific gene sets that were significantly enriched for the Q_{192} 0.85 mg/kg/d versus the control (acetone only) contrast, or membership in a WGCNA module. Samples used for qPCR validation included the 194 individual fetal brain samples that comprised the 60 pools used for microarray analysis, as well as the remaining 70 fetal brain samples from 20 dams that were not used for the microarray analysis. Each of the 264 samples were analyzed with a Fluidigm-based qPCR assay, using a 96.96 Dynamic Array Integrated Fluidic Circuit BioMark HD System (Fluidigm, San Francisco, CA) with an internal control for each gene spiked in at various dilutions to generate a standard curve that was used to estimate copy number. Copy number data were then normalized to a housekeeping gene, *β-actin*, and converted to

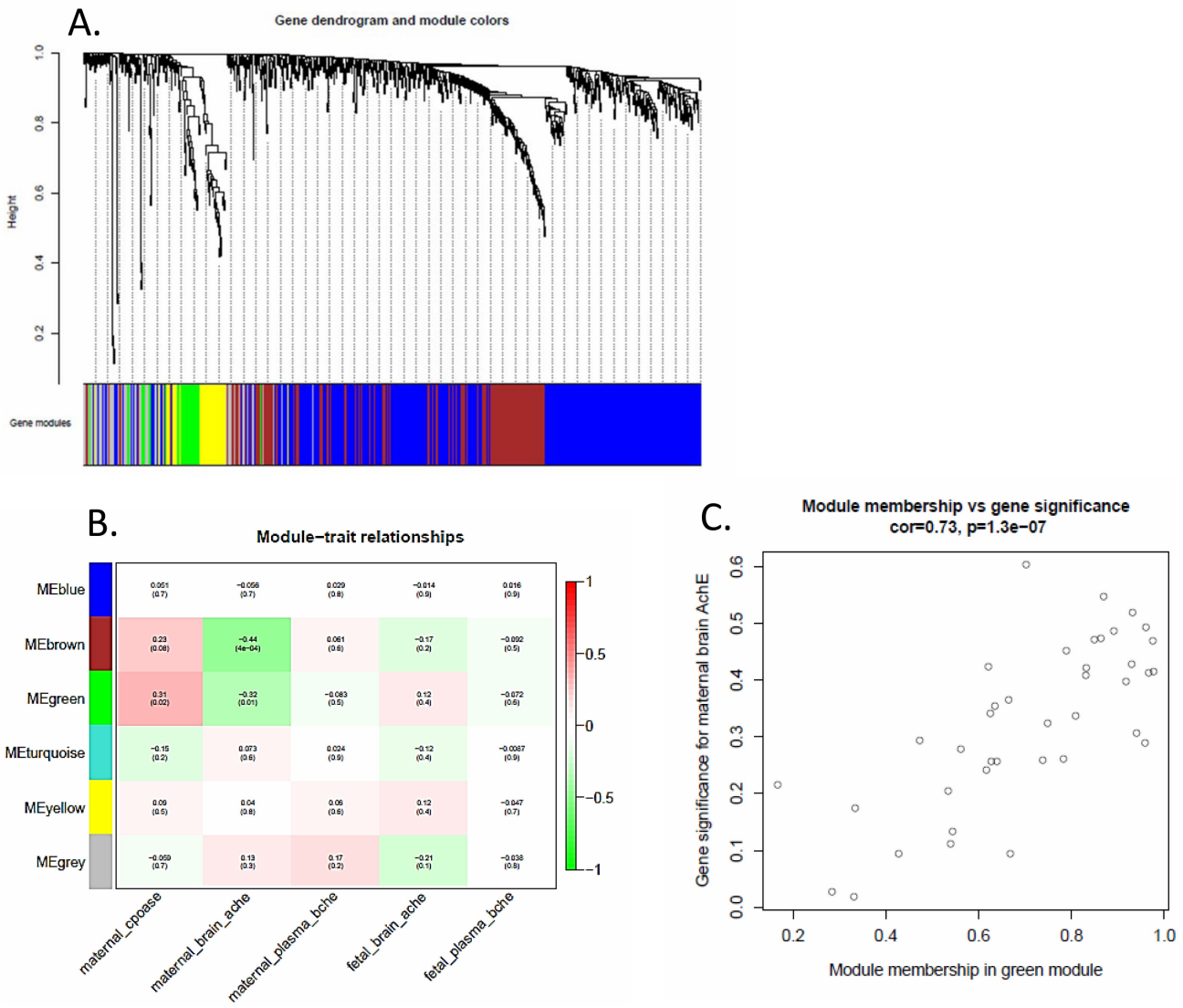

FIG. 1. Weighted Gene Coexpression Analysis (WGCNA). A) Hierarchical clustering showing the 6 gene modules (blue, brown, green, turquoise, yellow, grey) identified by WGCNA in fetal brain following gestational CPO exposure. B) Table showing the correlation of gene expression in the 6 gene modules with maternal plasma CPOase activity and with maternal and fetal brain and plasma AChE and BChE activity. C) Graph showing the highly significant correlation between module membership in the green module and gene significance for maternal brain AChE. The green module consisted of 39 genes, of which 11 were members of the HOX family.

$\log_2$ values. *β-Actin* expression was not affected by CPO exposure. Microarray data were compared with qPCR data in aggregate using X-Y plots for each contrast (not shown) and also by plotting comparisons of the fold changes of expression measured by qPCR and microarray for selected genes.

RESULTS

Maternal and Fetal PON1 Activity Levels

We determined maternal and fetal plasma PON1 activity levels by measuring rates of CPO hydrolysis. No significant differences in plasma CPOase activity were found between control and treated dams in any of the four genotypes (Table 2). Fetuses of *PON1*$^{+/+}$, *tgHuPON1*$_{R192}$, and *tgHuPON1*$_{Q192}$ had limited plasma CPOase activity. Fetal plasma PON1 activity was approximately 2–5% of maternal PON1 level in *tgHuPON1*$_{R192}$ and *tgHuPON1*$_{Q192}$ mice and 7% in *PON1*$^{+/+}$ mice. *PON1*$^{-/-}$ fetuses had no detectable plasma CPOase activity. Interestingly, *tgHuPON1*$_{R192}$ and *tgHuPON1*$_{Q192}$ dams had significantly higher plasma CPOase activity than *PON1*$^{+/+}$ dams (Table 2), but their liver microsomal CPOase activity was much lower, showing only 10–25% of the *PON1*$^{+/+}$ level (Table 3).

Maternal and Fetal Body Weights and Birth Outcomes

Our previous studies have shown that *PON1*$^{-/-}$ mice are much more sensitive to CPO toxicity than *PON1*$^{+/+}$ and human *PON1*-transgenic mice (Cole *et al.*, 2005; Shih *et al.*, 1998). To avoid overt toxicity, pregnant *PON1*$^{-/-}$ mice were treated with lower doses of CPO (0.5 and 0.75 mg/kg/day) compared with other genotypes (0.75 and 0.85 mg/kg/day). None of the treated dams showed any cholinergic signs during the 12-day-long treatment from GD6 to GD17. *PON1*$^{-/-}$ dams that received 0.75 mg/kg/day of CPO showed significantly lower body weight gain at GD18 (Table 1), and the effect remained unchanged after maternal body weight gain was adjusted for litter weight (litter weight was subtracted from the weight of the dam). Fetuses of the treated (0.75

TABLE 2. Maternal and Fetal Plasma Chlorpyrifos-Oxonase (CPOase) Activity Levels

	$PON1^{+/+}$		$PON1^{-/-}$		$tgHuPON1_{R192}$		$tgHuPON1_{Q192}$	
CPO (mg/kg/day)	Dams (units/l)	Fetuses (units/l)	Dams (units/l)	Fetuses (units/l)	Dams (units/l)	Fetuses (units/l)	Dams (units/l)	Fetuses (units/l)
0	1175 ± 202	75 ± 7	69 ± 2*	N.D.	2814 ± 80*	109 ± 10#	2840 ± 409*	26 ± 6#
0.5	–	–	72 ± 2*	N.D.	–	–	–	–
0.75	1274 ± 124	81 ± 9	72 ± 2*	N.D.	2823 ± 69*	115 ± 15	3434 ± 590*	68 ± 18
0.85	1421 ± 120	88 ± 10	–	–	2959 ± 128*	141 ± 13#	3974 ± 798*	59 ± 13

Notes. Data are presented as mean ± SE; $n = 5$–10 of each group; N.D. = Not detected.
Unit is defined as μmol of 3,5,6-TCP produced per minute.
No significant difference between treatment and control groups within each genotype.
*$p < 0.05$ as compared with $PON1^{+/+}$ dams; #$p < 0.05$ as compared with $PON1^{+/+}$ fetuses.

TABLE 3. Maternal Liver Microsomal Chlorpyrifos-Oxonase Activity Levels

	Microsomal chlorpyrifos-oxonase activity (units/g of protein)			
CPO (mg/kg/day)	$PON1^{+/+}$	$PON1^{-/-}$	$tgHuPON1_{R192}$	$tgHuPON1_{Q192}$
0	345 ± 33	N.D.	50 ± 4*	64 ± 3*
0.5	–	N.D.	–	–
0.75	333 ± 30	N.D.	37 ± 11*	72 ± 8*
0.85	362 ± 1	–	39 ± 5*	72 ± 10*

Notes. Data are presented as mean ± SE; $n = 3$–4 of each group; N.D. = Not detected.
Unit is defined as μmol of 3,5,6-TCP produced per minute.
No significant difference between treatment and control groups within each genotype.
*$p < 0.05$ as compared with $PON1^{+/+}$.

mg/kg/day) $PON1^{-/-}$ dams also showed decreased average body weights compared with vehicle controls (0.918 ± 0.021 vs. 1.043 ± 0.035; $p < 0.05$). On the other hand, CPO treatment did not cause any adverse effects on dams or birth outcomes in $PON1^{+/+}$, $tgHuPON1_{R192}$, or $tgHuPON1_{Q192}$ mice.

Both transgenic lines showed genotype-specific but treatment-independent differences in either maternal body weights or birth outcomes. Compared with other genotypes, $tgHuPON1_{R192}$ dams had an overall higher resorption rate. The $tgHuPON1_{Q192}$ dams had lower adjusted body weight gain, regardless of CPO treatment (Table 1).

Inhibition of Plasma BChE and CES Activities

All treated dams showed significant inhibition of plasma BChE activity, ranging from 30% to 50% (Fig. 2A). Gestational exposure to CPO did not cause BChE inhibition in $PON1^{+/+}$ or $tgHuPON1_{R192}$ fetuses; however, $PON1^{-/-}$ and $tgHuPON1_{Q192}$ fetuses were much more susceptible to CPO toxicity, showing significant decreases in plasma BChE activity (Fig. 2B). CES is a serine esterase that is abundant in mouse plasma and acts as a scavenger for OP compounds. CPO treatment caused moderate inhibition of plasma CES in all dams except $tgHuPON1_{Q192}$ mice (Fig. 3A). Plasma CES activity in $PON1^{-/-}$ fetuses was also significantly inhibited by CPO exposure (Fig. 3B).

Inhibition of Brain AChE

Maternal brain AChE activity of $PON1^{-/-}$, $tgHuPON1_{R192}$, and $tgHuPON1_{Q192}$ mice was significantly inhibited by approximately 50% following repeated CPO exposure (Fig. 4A). No inhibition of brain AChE activity was found in $PON1^{+/+}$ dams (Fig. 4A), even though they showed significant reduction of both plasma BChE (Fig. 2A) and CES activity (Fig. 3A). Effect on fetal brain AChE was found in $PON1^{-/-}$ fetuses only (Fig. 4B). Although $tgHuPON1_{R192}$ and $tgHuPON1_{Q192}$ dams showed increased sensitivity to CPO toxicity compared with $PON1^{+/+}$ dams, their fetuses were well protected from CPO exposure in terms of brain AChE activity (Fig. 4B).

Inhibition of Erythrocyte Acylpeptide Hydrolase

APH is a cytosolic enzyme found in a variety of tissues including brain, liver, and RBC. As a serine protease, APH of RBC is also a target enzyme for OP compounds and has been suggested to serve as a biomarker for OP exposure (Quistad *et al.*, 2005). We found that compared with other plasma target enzymes such as BChE and CES, APH of RBC was the most sensitive biomarker in dams following repeated exposure to CPO (Fig. 5A). Further, inhibition of APH activity by CPO exposure was genotype-dependent, with $PON1^{-/-}$ being the most sensitive, followed by $tgHuPON1_{Q192}$, $tgHuPON1_{R192}$, and $PON1^{+/+}$. However, no inhibition of APH activity was found in fetuses (Fig. 5B).

Gene Expression in the Fetal Brain

Gene expression in the brains of GD18 fetuses was measured using Affymetrix Mouse Gene 1.0 ST microarrays, followed by analysis of the expression data at the transcript level using RMA and a weighted ANOVA, with comparisons made among sample types by fitting empirical Bayes adjusted contrasts. Supplementary table 1 lists the probesets with unadjusted p values less than 0.05 and an absolute fold change of 1.5 or greater for the specific comparisons made between genotypes and treatment groups. Despite using an unadjusted p value of 0.05 as a measure of significance, there were still very few differentially expressed probesets for any of the contrasts, and many of the probesets did not correspond to known functionally annotated genes. Indeed,

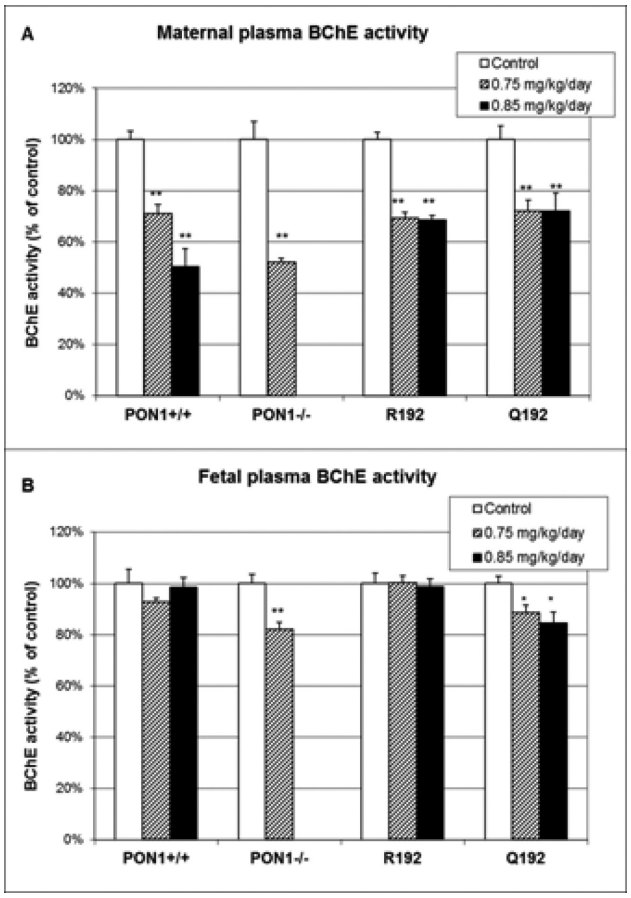

FIG. 2. Plasma BChE activity in dams (A) and fetuses (B). Pregnant $PON1^{+/+}$, $tgHuPON1_{R192}$, and $tgHuPON1_{Q192}$ mice were exposed to 0.75 mg/kg/day CPO, 0.85 mg/kg/day CPO, or vehicle alone from GD6 to GD17. $PON1^{-/-}$ dams were treated in the same manner but received lower doses of CPO of 0.5 mg/kg/day or 0.75 mg/kg/day. Dose-dependent plasma BChE inhibition was found in $PON1^{-/-}$ dams but only the group that received 0.75 mg/kg/day CPO was presented here. Plasma BChE activity was determined at GD18, 24 h after the last dosing of CPO. Data are presented as mean ± SE. $N = 5$–10 for each treatment group. $^{*}p < 0.05$ and $^{**}p < 0.01$ as compared with vehicle control.

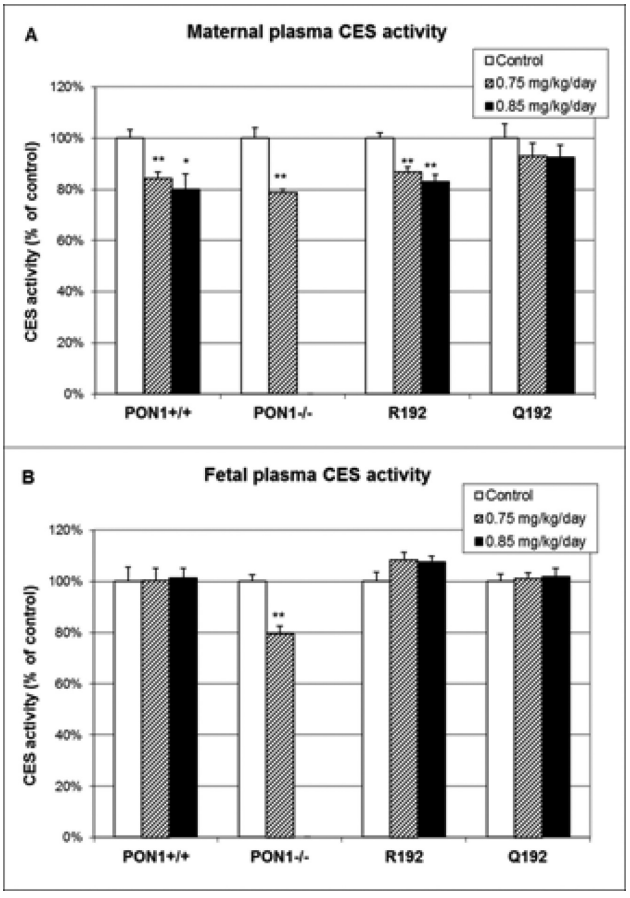

FIG. 3. Plasma CES activity in dams (A) and fetuses (B). Pregnant $PON1^{+/+}$, $tgHuPON1_{R192}$, and $tgHuPON1_{Q192}$ mice were exposed to 0.75 mg/kg/day CPO, 0.85 mg/kg/day CPO, or vehicle alone from GD6 to GD17. $PON1^{-/-}$ dams were treated in the same manner but received lower doses of CPO at 0.5 mg/kg/day and 0.75 mg/kg/day. Plasma CES activity was determined at GD18, using *p*-nitrophenyl valerate as substrate. Data are presented as mean ± SE. $N = 5$–10 for each treatment group. $^{*}p < 0.05$ and $^{**}p < 0.01$ as compared with vehicle control.

no known genes were differentially expressed in the treated versus control comparisons of $PON1^{+/+}$ or $PON1^{-/-}$ mice, and only one known gene (*triadin*) was affected in the $tgHuPON1Q_{192}$ comparisons. Furthermore, PCA did not reveal any particular grouping of data according to genotype or treatment (not shown). This may reflect either a high technical or biological variability, which may be masking true differences, or alternatively there may be many very small changes in gene expression that result in a visible phenotypic difference. To address the latter possibility, GSEA was used to detect statistically significant changes in expression for groups of genes in their entirety (rather than individual genes). To determine whether the phenotypic differences in maternal or fetal enzyme inhibition correlated with any particular groups of genes, WGCNA was performed.

Weighted Gene Coexpression Analysis

WGCNA uses the correlations between expression values to infer gene networks (Langfelder and Horvath, 2008). Figure 1A shows the clustering dendrogram generated by the initial WGCNA analysis. The colored bars at the bottom of the plot indicate the cluster boundaries for the five clusters (blue, brown, green, turquoise, and yellow) that were identified by this analysis. The gray band covers those genes that do not cluster. Supplementary table 2 lists the genes (blue, 401 genes; brown, 160 genes; green, 39 genes; turquoise, 225 genes; yellow, 45 genes; gray, 74 genes) that comprise each of these clusters. The gene clusters were then correlated with phenotypic data (maternal and fetal CPOase, brain AChE, plasma BChE, and plasma CES). Figure 1B shows a heat map illustrating the correlation and correlation *p* value between each cluster and phenotypic measure. The most notable pattern was the negative correlation between maternal brain AChE and the green gene module. In addition, there was a positive correlation between maternal plasma CPOase and the green module. Correlation values with phenotypic data for maternal and fetal brain AChE and plasma BChE are listed in Supplementary table 2 for each gene in the six clusters. To more closely examine the genes in the green gene module with respect to a given phenotype, Figure 1C plots module membership, which infers the importance of a gene to the module, versus gene significance, which measures the correlation between a given gene and the phenotypic measure, in this case maternal brain AChE. The correlation between these measures was quite high, and significant. The genes at the top right of the plot are those that are highly correlated to both maternal brain

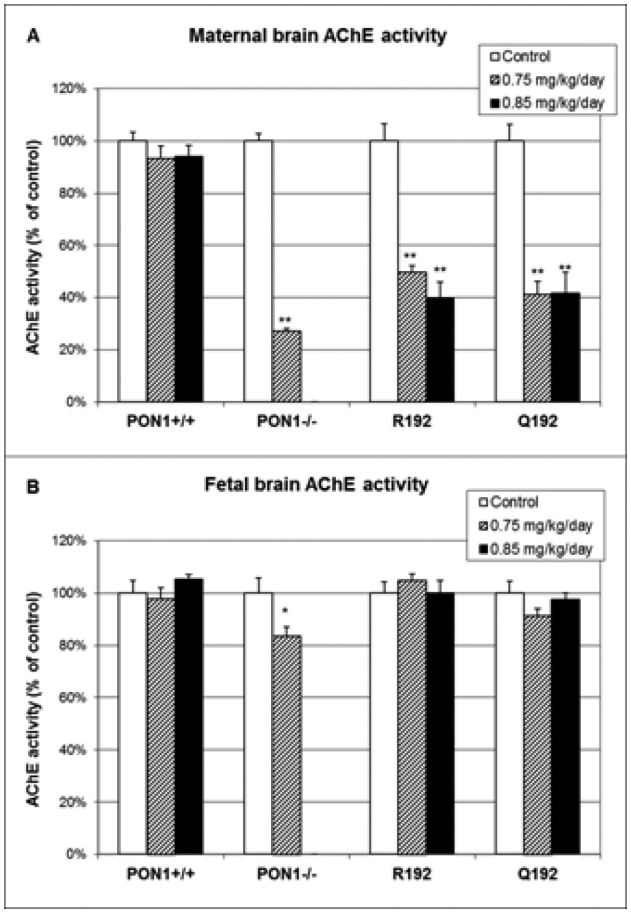

FIG. 4. Brain AChE activity in dams (A) and fetuses (B). Pregnant $PON1^{+/+}$, $tgHuPON1_{R192}$, and $tgHuPON1_{Q192}$ mice were exposed to 0.75 mg/kg/day CPO, 0.85 mg/kg/day CPO, or vehicle alone from GD6 to GD17. $PON1^{-/-}$ dams were treated in the same manner but received lower doses of CPO at 0.5 mg/kg/day and 0.75 mg/kg/day. Dose-dependent brain AChE inhibition was found in $PON1^{-/-}$ dams but only the group that received 0.75 mg/kg/day CPO was presented here. Brain AChE activity was determined at GD18 as described in the Materials and Methods section. Data are presented as mean ± SE. $N = 5$–10 for each treatment group. $^{*}p < 0.05$ and $^{**}p < 0.01$ as compared with vehicle control.

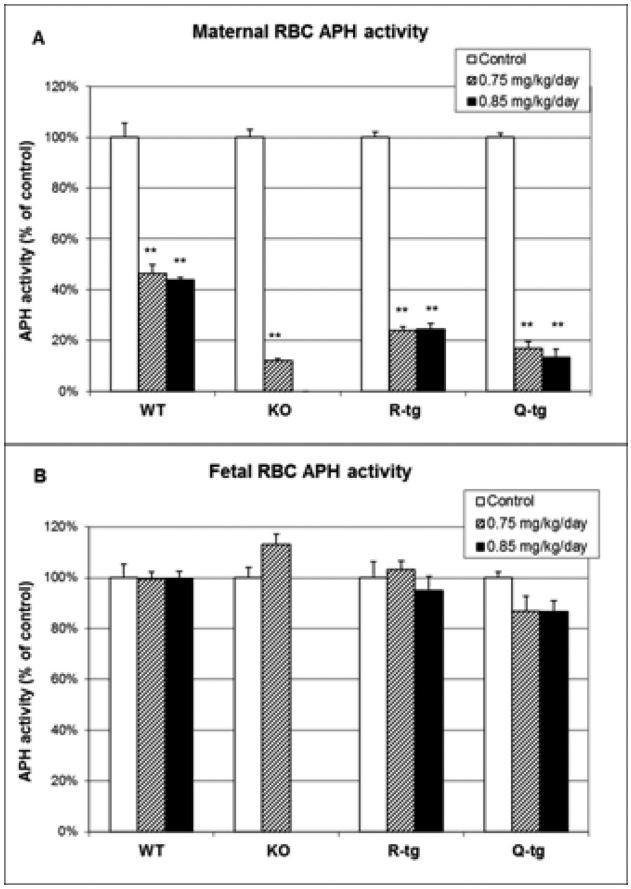

FIG. 5. RBC APH activity in dams (A) and fetuses (B). Pregnant $PON1^{+/+}$, $tgHuPON1_{R192}$, and $tgHuPON1_{Q192}$ mice were exposed to 0.75 mg/kg/day CPO, 0.85 mg/kg/day CPO, or vehicle alone from GD6 to GD17. $PON1^{-/-}$ dams were treated in the same manner but received lower doses of CPO at 0.5 mg/kg/day and 0.75 mg/kg/day. RBC APH activity was determined at GD18, using N-acetyl-L-alanyl-*p*-nitroanilide as substrate. Data are presented as mean ± SE. N = 5–10 for each treatment group. $^{*}p < 0.05$ and $^{**}p < 0.01$ as compared with vehicle control.

AChE levels, as well as being "hub" genes in the green module, with high inter-gene correlations with a preponderance of the other genes in this gene module. Interestingly, homeobox (HOX) genes comprised a large number of the genes in the green module, and HOX gene expression was negatively correlated with maternal brain AChE activity. Thus, AChE inhibition in the maternal brain was associated with an increase in HOX gene expression (and the expression of some other green module genes) in the brains of that dam's fetuses following repeated gestational CPO exposure.

Gene Set Enrichment Analysis

GSEA was performed using 14 different categories of BROAD Institute gene sets (GO Biological Process, GO Cellular Component, GO Molecular Function, Biocarta, Cancer Gene Neighborhood, Cancer Modules, Canonical Pathway, Chemical Genetic Perturbations, KEGG, MicroRNA, Oncogenic, Positional, Reactome, and Transcription Factor Targets). Significantly enriched gene sets were assessed for the treated versus control comparisons in each of the four genotypes, as well as for the between-genotype comparisons ($PON1^{+/+}$ vs. $PON1^{-/-}$ and $tgHuPON1_{Q192}$ vs. $tgHuPON1_{R192}$) of mice exposed to the same dose of CPO (0.75 mg/kg/d or 0.85 mg/kg/d).

Supplementary table 3 lists the gene sets that were significantly ($p < 0.05$) enriched ("up," "down," or "mixed" as indicated) in the treated versus control comparisons for each genotype, focusing on four gene set categories of particular interest (GO Cellular Component, GO Molecular Function, KEGG, and Reactome). A wide variety of gene sets were identified based on this analysis, including gene sets comprised of as few as 6 or as many as 1577 genes, and with p values as low as $p = 0.0001$. In all cases, there were more significantly enriched gene sets in the fetuses of $tgHuPON1_{Q192}$ dams compared with the fetuses of $tgHuPON1_{R192}$ dams. For example, for the 0.85 mg/kg/d versus control comparisons in transgenic mice, there were 24 ($tgHuPON1_{Q192}$) and 6 ($tgHuPON1_{R192}$) significantly enriched gene sets in the GO Cellular Component category, 42 ($tgHuPON1_{Q192}$) and 20 ($tgHuPON1_{R192}$) significantly enriched gene sets in the GO Molecular Function category, 28 ($tgHuPON1_{Q192}$) and 12 ($tgHuPON1_{R192}$) significantly enriched KEGG gene sets, and 77 ($tgHuPON1_{Q192}$) and 34 ($tgHuPON1_{R192}$) significantly enriched Reactome gene sets (Supplementary table 3).

Supplementary table 4 lists the gene sets in these same categories (GO Cellular Component, GO Molecular Function,

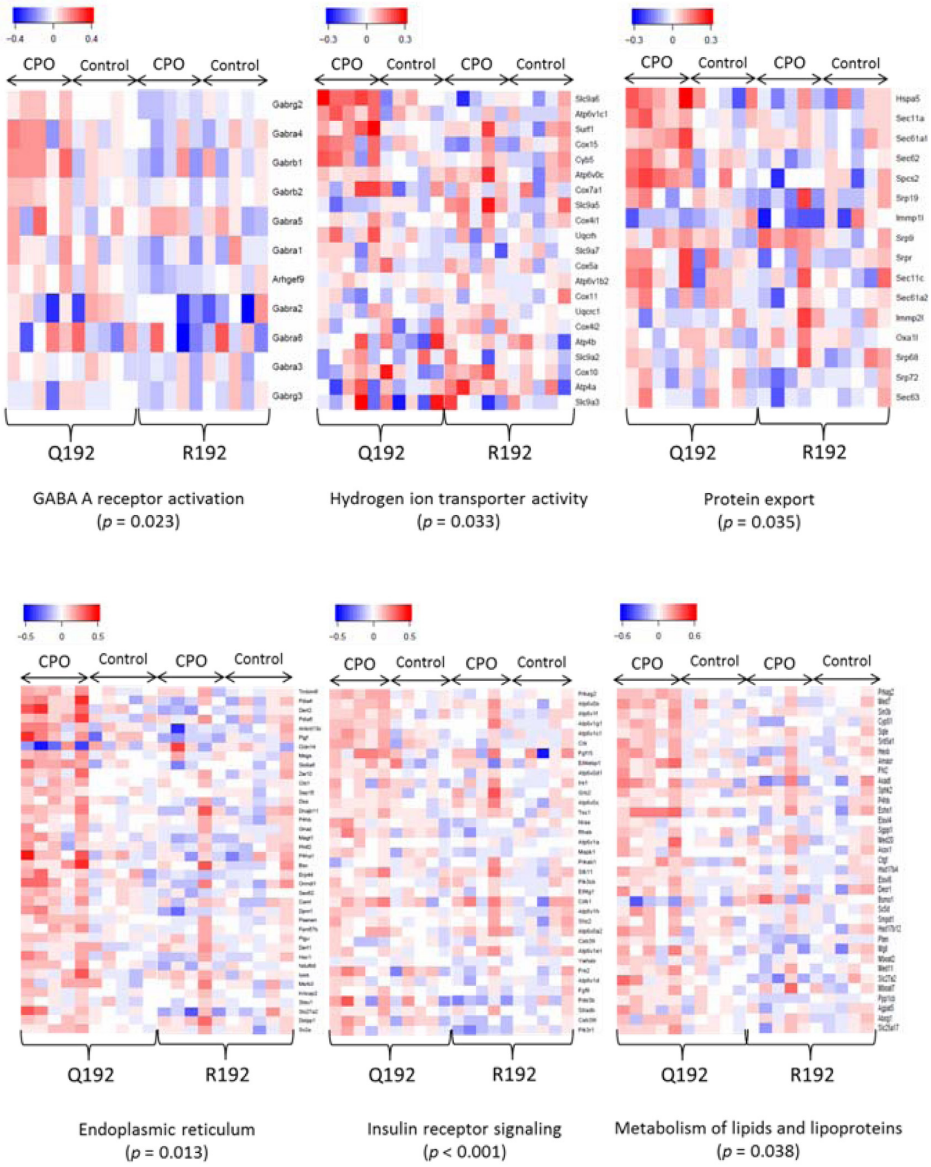

FIG. 6. GSEA heat maps. Heat maps of some gene sets of particular interest that were significantly ($p < 0.05$) enriched in the brains of *tgHuPON1*$_{Q192}$ fetuses from CPO-treated (0.85 mg/kg/d) dams compared with fetuses from vehicle-treated dams. Heat maps are shown for *tgHuPON1*$_{Q192}$ mice (Q192; on the left of each heat map) and *tgHuPON1*$_{R192}$ mice (R192; on the right of each heat map) exposed to 0.85 mg/kg/d CPO ("CPO") or to vehicle ("Control"). Rows correspond to individual genes. Columns correspond to pooled fetal-brain samples from each dam. Red color indicates increased expression. Blue color indicates decreased expression.

KEGG, Reactome) that were significantly ($p < 0.05$) enriched for the between-genotype comparisons of *tgHuPON1*$_{Q192}$ and *tgHuPON1*$_{R192}$ mice (*tgHuPON1*$_{Q192}$ 0.85 mg/kg/d vs. *tgHuPON1*$_{R192}$ 0.85 mg/kg/d; *tgHuPON1*$_{Q192}$ 0.75 mg/kg/d vs. *tgHuPON1*$_{R192}$ 0.75 mg/kg/d) or of *PON1*$^{-/-}$ and *PON1*$^{+/+}$ mice (*PON1*$^{-/-}$ 0.75 mg/kg/d vs. *PON1*$^{+/+}$ 0.75 mg/kg/d). For the high-dose (0.85 mg/kg/d) comparison between *tgHuPON1*$_{Q192}$ and *tgHuPON1*$_{R192}$ mice, there were 5 GO Cellular Component gene sets, 34 GO Molecular Function gene sets, 14 KEGG gene sets, and 35 Reactome gene sets that were significantly enriched (Supplementary table 4). At the low dose (0.75 mg/kg/d), there were 27 GO Cellular Component gene sets, 22 GO Molecular Function gene sets, 32 KEGG gene sets, and 86 Reactome gene sets that were significantly enriched in the comparison between *tgHuPON1*$_{Q192}$ and *tgHuPON1*$_{R192}$ mice (Supplementary table 4). Comparison of *PON1*$^{-/-}$ and *PON1*$^{+/+}$ mice exposed to 0.75 mg/kg/d CPO revealed 15 GO Cellular Component gene sets, 23 GO Molecular Function gene sets, 13 KEGG gene sets, and 58 Reactome gene sets that were significantly enriched (Supplementary table 4).

Figure 6 shows heat maps of six selected gene sets identified by GSEA that were significantly enriched ($p < 0.05$) in the brains of *tgHuPON1*$_{Q192}$ offspring treated with 0.85 mg/kg/d of CPO compared with vehicle, in comparison with the heat maps of the same gene sets from the brains of *tgHuPON1*$_{R192}$ offspring. All of the heat maps showed stronger effects in terms of gene expression differences in the *tgHuPON1*$_{Q192}$ offspring compared with the *tgHuPON1*$_{R192}$ offspring. Among the six gene sets, one Reactome gene set (GABA A Receptor Reaction) was also significantly enriched for the direct between-genotype comparison of *tgHuPON1*$_{Q192}$ versus *tgHuPON1*$_{R192}$ offspring exposed to 0.85 mg/kg/d CPO.

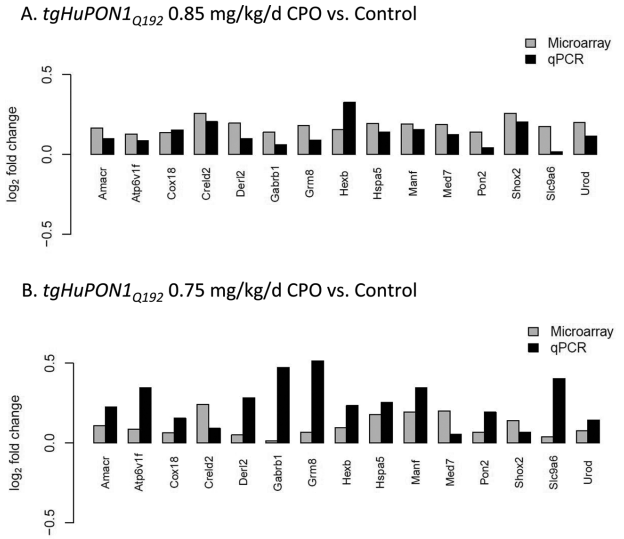

FIG. 7. Validation by qPCR. Comparison of the $\log_2$ fold change of expression of selected genes, as measured by microarray (light bars) and qPCR (dark bars), in *tgHuPON1*$_{Q192}$ mice for (A) 0.85 mg/kg/d CPO versus control contrast and (B) 0.75 mg/kg/d CPO versus control contrast.

RT-PCR Confirmation

Thirty genes were selected for validation by qPCR based on the high dose (0.85 mg/kg/d) versus control contrast in *tgHuPON1*$_{Q192}$ mice. About two-thirds of these were based on gene sets that were significant in aggregate, and the other one-third were selected based on *p* value and fold change from the original univariate comparisons. Specific genes selected for confirmation by qPCR are listed in Table 4. Samples were analyzed with a Fluidigm-based qPCR assay, normalizing the copy number data to the housekeeping gene, *β-actin*. Figure 7 shows the $\log_2$ fold change of expression, as measured by microarray (light bars) and qPCR (dark bars), of the genes (*Amacr, Atp6v1f, Cox18, Creld2, Derl2, Gabrb1, Grm8, Hexb, Hspa5, Manf, Med7, Pon2, Shox2, Urod*) for which microarray expression values were validated by qPCR. These genes showed good correspondence between the microarray and qPCR data, with $\log_2$ fold-change values ranging from approximately + 0.2 to + 0.5.

DISCUSSION

This study shows that gestational exposure to CPO causes cholinesterase (ChE) inhibition in fetuses and alterations of gene expression in fetal brain. These effects are modulated by maternal PON1 status, with *PON1*$^{-/-}$ fetuses being the most susceptible to CPO toxicity and *tgHuPON1*$_{Q192}$ fetuses being more sensitive to CPO than *tgHuPON1*$_{R192}$ fetuses. This is the first study using a humanized transgenic mouse model to demonstrate that maternal PON1 activity levels as well as the genotype of maternal PON1$_{Q192R}$ polymorphism modulate the toxic effects of OP exposure during pregnancy. In this study, dams were exposed to the toxic oxon CPO, instead of the parent compound CPS. However, given the presence of CPO in most exposures including air samples and crops (Armstrong *et al.*, 2013a,b; Vidal *et al.*, 1998), the importance of direct exposure to CPO cannot be ignored, even for the general population. The doses of CPO used in the present study caused only moderate or no inhibition of maternal ChE in *PON1*$^{+/+}$ mice but had severe effects in genetically compromised *PON1*$^{-/-}$ and *tgHuPON1*$_{Q192}$ mice, reflecting the nature of genetic variability and susceptibility in humans. Our results are in agreement with previous epidemiologic studies that reported a positive association between developmental delay in children and *in utero* exposure to OP insecticides, particularly in children whose mothers were homozygous for the Q_{192} allele or had low serum PON1 activity levels (Berkowitz *et al.*, 2004; Engel *et al.*, 2011; Eskenazi *et al.*, 2010).

Plasma PON1 activity levels are extremely low in fetuses (Table 2), indicating that fetuses have little ability to hydrolyze CPO and must depend on maternal biotransformation enzymes to detoxify the compound before it reaches the fetus. It is known that fetuses recover rapidly from the inhibitory effect of CPO on brain AChE and plasma BChE due to the rapid *de novo* synthesis of these enzymes in the fetus (Ashry *et al.*, 2002). Despite this rapid recovery, we still found significant inhibition of plasma BChE in both *PON*$^{-/-}$ and *tgHuPON1*$_{Q192}$ fetuses and inhibition of brain AChE in *PON*$^{-/-}$ fetuses. These findings suggest that without the protection afforded by a catalytically efficient maternal PON1, i.e., the PON1$_{R192}$ alloform, fetuses cannot recover from repeated exposure to CPO. A previous study in C57BL/6 mice with a similar design of gestational exposure (GD6 to GD17, s.c.) but using the parent compound CPS also showed that fetuses were more resistant to CPS toxicity than dams (Moreira *et al.*, 2010). In that study, CPS doses of 10–15 mg/kg/d inhibited maternal and fetal brain AChE by 40–60% and 20–30%, respectively. In contrast, CPO doses of 0.75–0.85 mg/kg/d in the current study inhibited maternal brain AChE in the humanized transgenic mice by about the same amount (50–60%), but there was no inhibition of fetal brain AChE. This increased sensitivity of fetal brain AChE to CPS compared with CPO is likely due to rapid detoxication of CPO in the maternal plasma, whereas CPS may undergo more localized biotransformation to CPO in the fetus or placenta. Compared with *PON1*$^{+/+}$ dams, *tgHuPON1*$_{R192}$ and *tgHuPON1*$_{Q192}$ dams had relatively low levels of liver PON1 activity (Table 3). In this study, it appears that maternal liver PON1 may not play a significant role in modulating CPO toxicity in the fetus because even with very low liver PON1 activity levels, *tgHuPON1*$_{R192}$ dams offered sufficient protection for their fetuses. In addition to plasma PON1, maternal plasma BChE and CES may also provide some protection against CPO by covalently binding CPO.

An interesting finding of this study is that RBC APH seemed to be a more sensitive biomarker in dams than plasma BChE following repeated CPO exposure. In the dams, RBC APH was inhibited to a greater extent than plasma BChE in all genotypes of mice. For example, when *tgHuPON1*$_{Q192}$ dams were exposed to 0.85 mg/kg/d of CPO for 12 days, their RBC APH was inhibited to 13% of control whereas plasma BChE was 72% of control. The much higher inhibition found in RBC APH could be due to a longer half-life of RBC APH than plasma BChE (33 days vs. 11 days). The strong inhibitory effect on APH is of great interest because brain APH was found to function in cleavage of β-amyloid peptide (Yamin *et al.*, 2007) and modulation of synaptic plasticity (Olmos *et al.*, 2009), and this mechanism may be relevant to the effects of CPO exposure on expression of gene sets related to neurodegenerative disease and neurotransmission. It has been suggested that RBC APH can be used as an alternative biomarker for OP exposure (Quistad *et al.*, 2005) and our related study also shows a good correlation of RBC APH inhibition with diazinon-oxon toxicity in brain and diaphragm (Li *et al.*, in preparation).

Another interesting finding is that compared with other genotypes, *tgHuPON1*$_{R192}$ dams tended to have a high resorption rate (number of resorptions per implant) regardless of CPO exposure (Table 1). It is unclear why *tgHuPON1*$_{R192}$ mice had a relatively high resorption rate. However, a recent epidemiologic

TABLE 4. Genes Selected and Confirmed by RT-PCR

Symbol	Gene description	Selection criteria	RT-PCR confirmation	*p* value	$\log_2$ fold change
Derl2	Derlin-2	GSEA: GO_CC_Endoplasmic_Reticulum	Yes	0.0026	0.1961
Slc9a6	Solute carrier family 9 (Na^+/H^+ exchanger) member a6	GSEA: GO_CC_Endoplasmic_Reticulum	Yes	0.0128	0.1754
Cox18	COX18 cytochrome c oxidase assembly homolog	GSEA: GO_CC_Mitochondrial_Inner_Membrane	Yes	0.0074	0.1356
Ndufb2	NADH dehydrogenase (ubiquinone) 1 β subcomplex 2	GSEA: KEGG_Oxidative_Phosphorylation	Yes	0.0451	0.1740
Hspa5	Heat shock protein 5	GSEA: KEGG_Protein_Export	Yes	0.0018	0.1943
Gabrb1	γ-Aminobutyric acid (GABA) A receptor, subunit β 1	GSEA: Reactome_GABA_A_Receptor_Activation	Yes	0.0121	0.1386
Amacr	α-Methylacyl-CoA racemase	GSEA: Reactome_Metabolism_Of_Lipids_And_Lipoproteins	Yes	0.0091	0.1656
Hexb	Hexosaminidase B	GSEA: Reactome_Metabolism_Of_Lipids_And_Lipoproteins	Yes	0.0076	0.1553
Med7	Mediator complex subunit 7	GSEA: Reactome_Metabolism_Of_Lipids_And_Lipoproteins	Yes	0.0023	0.1866
Atp6v1f	ATPase, H+ transporting, lysosomal V1 subunit F	GSEA: Reactome_Signaling_By_Insulin_Receptor	Yes	0.0088	0.1282
Pon2	Paraoxonase 2	Gene of particular interest (Paraoxonase)	Yes	0.0292	0.1405
Creld2	Cysteine-rich with EGF-like domain 2	*p* value/fold change	Yes	0.0011	0.2581
Grm8	Glutamate receptor, metabotropic 8	*p* value/fold change	Yes	0.0076	0.1553
Manf	Mesencephalic astrocyte-derived neurotrophic factor	*p* value/fold change	Yes	0.0006	0.1909
Shox2	Short stature homeobox 2	*p* value/fold change	Yes	0.0001	0.2570
Urod	Uroporphyrinogen decarboxylase	*p* value/fold change	Yes	0.0008	0.2009
Pdia4	Protein disulfide isomerase associated 4	GSEA: GO_CC_Endoplasmic_Reticulum	No	0.0018	0.1916
Ndufa13	NADH dehydrogenase (ubiquinone) 1 α subcomplex 13	GSEA: GO_CC_Mitochondrial_Inner_Membrane	No	0.0077	0.1361
Ndufa4	NADH dehydrogenase (ubiquinone) 1 α subcomplex 4	GSEA: KEGG_Oxidative_Phosphorylation	No	0.0127	0.1698
Ndufab1	NADH dehydrogenase (ubiquinone) 1 α/β subcomplex 1	GSEA: KEGG_Oxidative_Phosphorylation	No	0.0003	0.1549
Ndufb6	NADH dehydrogenase (ubiquinone) 1 β subcomplex 6	GSEA: KEGG_Oxidative_Phosphorylation	No	0.0074	0.2229
Uqcrfs1	Ubiquinol-cytochrome c reductase, Rieske iron-sulfur polypeptide 1	GSEA: KEGG_Oxidative_Phosphorylation	No	0.0146	0.1523

TABLE 4. Continued

Symbol	Gene description	Selection criteria	RT-PCR confirmation	*p* value	$\log_2$ fold change
Mgat3	Mannoside acetyl-glucosaminyltrans-ferase 3	GSEA: Reactome_Glutamate_Neurotransmitter_Release_Cycle	No	0.0037	0.1653
Cyp51	Cytochrome P450, family 51	GSEA: Reactome_Metabolism_Of_Lipids_And_Lipoproteins	No	0.0043	0.1355
Prkag2	Protein kinase, AMP-activated, γ-2 non-catalytic subunit	GSEA: Reactome_Metabolism_Of_Lipids_And_Lipoproteins	No	0.0005	0.1254
Srd5a1	Steroid 5 alpha reductase 1	GSEA: Reactome_Metabolism_Of_Lipids_And_Lipoproteins	No	0.0046	0.1444
Gpr137b	G protein-coupled receptor 137B	*p* value/fold change	No	0.0001	0.2529
L2hgdh	L-2-hydroxyglutarate dehydrogenase	*p* value/fold change	No	0.0008	0.3494
Mtfp1	Mitochondrial fission process 1	*p* value/fold change	No	0.0014	0.2262
Tubd1	Tubulin, delta 1	*p* value/fold change	No	0.0015	0.2050

Notes. "*p* value/fold change": Selected genes with *p* values < 0.01 and $\log_2$ fold change > 0.15 that were determined to be of particular interest. No RT-PCR genes were from the WGCNA analysis.
For genes selected on the basis of GSEA, the gene set listed is that with the most significant enrichment.

study showed that the risk of miscarriage by $PON1_{R192}$ homozygous women was 2.2 times higher than women of QR and QQ genotypes (Blanco-Munoz *et al.*, 2013). What possible explanation is behind the high rate of resorption/miscarriage found to be associated with the $PON1_{R192}$ allele is worthy of additional studies.

The microarray data reported in the current study are consistent with increased sensitivity to CPO of individuals carrying the $tgHuPON1_{Q192}$ alloform. As in our previous study that examined gene expression following neonatal exposure to CPO (Cole *et al.*, 2011), individual gene analysis revealed only a small number of affected genes. This was not surprising given the low doses of CPO used for the study and signal dilution due to the use of the entire fetal brain and pooling of the samples, therefore, WGCNA and GSEA were used as more sensitive methods to investigate the subtle gene expression effects following gestational CPO exposure.

WGCNA allowed anchoring of the gene expression effects to the phenotypic data on biomarker inhibition and plasma PON1 levels. WGCNA identified six gene modules based on clustering of the correlations among their fetal-brain expression values. The "green" module, which correlated highly with maternal plasma CPOase activity and negatively with maternal brain AChE activity, had a large representation (11/39 genes) of HOX genes, suggesting effects of gestational CPO exposure on axial patterning during development that are correlated with the ability of maternal PON1 levels to protect against brain AChE inhibition.

Due to the smaller effect sizes associated with low-level CPO exposure, GSEA was used to evaluate the expression of gene sets, using 14 different categories from the BROAD Institute (http://www.broadinstitute.org/gsea/msigdb/index.jsp). In all of the categories, there were more significantly enriched gene sets in the fetuses of $tgHuPON1_{Q192}$ dams compared with those of $tgHuPON1_{R192}$ dams, consistent with the lower catalytic efficiency of the $PON1_{Q192}$ alloform for hydrolyzing CPO. Supplementary table 3 lists a large number of gene sets in several different categories that were enriched in the $tgHuPON1_{Q192}$ mice following CPO exposure. In addition to the gene sets whose heat maps are shown in Figure 6 (GABA-A receptor activation, lipid metabolism, protein export, endoplasmic reticulum, hydrogen ion transporter activity, and insulin receptor signaling), gene sets identified include those related to the mitochondrial respiratory chain, the cell cycle, vesicle membranes, neurotransmission by glutamate receptors, and Wnt signaling, among many others. To our knowledge, there have only been two studies examining gene expression in the brains of mice following developmental OP exposure (Cole *et al.*, 2011; Moreira *et al.*, 2010), and both offer an interesting comparison with the current study. Moreira *et al.* (2010) exposed C57BL/6 mice to five different doses of CPS over the same gestational period used in the current study, producing similar levels of maternal brain AChE inhibition. They also measured gene expression in pooled GD18 fetal brains using Affymetrix Mouse Genome arrays. Some of the GO Biological Process categories they identified were similar to the gene sets identified in the current study, including GO categories related to the cell cycle, lipid biosynthesis and transport, vesicle-mediated transport, neurotransmission, Wnt and MAPK signaling, ER-related signaling, growth regulation, and nervous system development, as well as KEGG pathways that included neurodegenerative diseases and insulin signaling (Moreira *et al.*, 2010). Nervous system development, synaptic transmission, and Wnt signaling were also identified as relevant pathways in the adult rat forebrain by Stapleton and Chan (2009). Wnt signaling was also affected in neonatal rat (Slotkin *et al.*, 2008). The only other study to assess CPO effects on gene expression was by Cole *et al.* (2011) in which mice were exposed to CPO neonatally and gene expression was measured in the cerebellum at PND22. Some of the gene sets identified in the postnatal study were similar to the ones recognized in the current study, including those related to the mitochondrial respiratory chain, synaptic transmission, insulin receptor signaling, MAPK signaling, lipid metabolism, and oxidoreductase activity (Cole *et al.*, 2011). As in the current study, Cole *et al.* (2011) found that mice expressing $tgHuPON1_{Q192}$ were

more sensitive to CPO-related effects on gene expression than mice expressing *tgHuPON1*$_{R192}$.

This is the first and the only study in an animal model that addresses the differential susceptibility to CPO afforded by the *tgHuPON1*$_{Q192R}$ polymorphism during pregnancy. The data show that maternal PON1 status modulates the effects of repeated gestational CPO exposure on enzyme activities in the dam and fetuses, and gene expression measured in the GD18 fetal brain. Consistent with previous studies both in adults and during development (Cole *et al.*, 2005, ;2011; Li *et al.*, 2000), the *tgHuPON1*$_{Q192}$ alloform was less protective than *tgHuPON1*$_{R192}$ against CPO exposure. It must be noted that in the current study, dams of the same genotype and treatment group expressed similar PON1 levels; however, plasma PON1 activity levels vary by at least 13-fold among individuals (Furlong *et al.*, 2006) and therefore it is important to also measure PON1 activity within each PON1$_{192}$ genotype in epidemiologic studies.

SUPPLEMENTARY DATA

Supplementary data are available online at http://toxsci.oxfordjournals.org/.

FUNDING

National Institute of Environmental Health Sciences (P42-ES04696, U19-ES11387, P30-ES07033, R01-ES09883, and R01-ES09601]; The Center on Human Development and Disability (P30-HD02274); United States Environmental Protection Agency (R826886).

ACKNOWLEDGMENTS

The authors thank the technical staff at the UW Functional Genomics and Bioinformatics Laboratory for assistance with RNA isolation and quality control, and members of the Furlong, Costa, and Faustman laboratories for helpful discussions and technical support. The transgenic and knockout mouse lines were kindly provided by Dr. Aldons J. Lusis, Dr. Diana Shih, and Dr. Aaron Tward at UCLA.

REFERENCES

Armstrong, J. L., Fenske, R. A., Yost, M. G., Galvin, K., Tchong-French, M. and Yu, J. (2013a). Presence of organophosphorus pesticide oxygen analogs in air samples. *Atmos. Environ.* **66**, 145–150.

Armstrong, J. L., Fenske, R. A., Yost, M. G., Tchong-French, M. and Yu, J. (2013b). Comparison of polyurethane foam and XAD-2 sampling matrices to measure airborne organophosphorus pesticides and their oxygen analogs in an agricultural community. *Chemosphere* **92**, 451–457.

Ashry, K. M., Abu-Qare, A. W., Saleem, F. R., Hussein, Y. A., Hamza, S. M., Kishk, A. M. and Abou-Donia, M. B. (2002). Inhibition and recovery of maternal and fetal cholinesterase enzymes following a single oral dose of chlorpyrifos in rats. *Arch. Toxicol.* **76**, 30–39.

Berkowitz, G. S., Wetmur, J. G., Birman-Deych, E., Obel, J., Lapinski, R. H., Godbold, J. H., Holzman, I. R. and Wolff, M. S. (2004). In utero pesticide exposure, maternal paraoxonase activity, and head circumference. *Environ. Health Perspect.* **112**, 388–391.

Betancourt, A. M., Burgess, S. C. and Carr, R. L. (2006). Effect of developmental exposure to chlorpyrifos on the expression of neurotrophin growth factors and cell-specific markers in neonatal rat brain. *Toxicol. Sci.* **92**, 500–506.

Blanco-Munoz, J., Aguilar-Garduno, C., Gamboa-Avila, R., Rodriguez-Barranco, M., Perez-Mendez, O., Huesca-Gomez, C., Gonzalez-Alzaga, B. and Lacasana, M. (2013). Association between PON1 genetic polymorphisms and miscarriage in Mexican women exposed to pesticides. *Sci. Total Environ.* **449**, 302–308.

Bouchard, M. F., Chevrier, J., Harley, K. G., Kogut, K., Vedar, M., Calderon, N., Trujillo, C., Johnson, C., Bradman, A., Barr, D. B., *et al.* (2011). Prenatal exposure to organophosphate pesticides and IQ in 7-year-old children. *Environ. Health Perspect.* **119**, 1189–1195.

Brazma, A., Hingamp, P., Quackenbush, J., Sherlock, G., Spellman, P., Stoeckert, C., Aach, J., Ansorge, W., Ball, C. A., Causton, H. C., *et al.* (2001). Minimum information about a microarray experiment (MIAME)-toward standards for microarray data. *Nat. Genet.* **29**, 365–371.

Cole, T. B., Beyer, R. P., Bammler, T. K., Park, S. S., Farin, F. M., Costa, L. G. and Furlong, C. E. (2011). Repeated developmental exposure of mice to chlorpyrifos oxon is associated with paraoxonase 1 (PON1)-modulated effects on cerebellar gene expression. *Toxicol. Sci.* **123**, 155–169.

Cole, T. B., Jampsa, R. L., Walter, B. J., Arndt, T. L., Richter, R. J., Shih, D. M., Tward, A., Lusis, A. J., Jack, R. M., Costa, L. G., *et al.* (2003). Expression of human paraoxonase (PON1) during development. *Pharmacogenetics* **13**, 357–364.

Cole, T. B., Walter, B. J., Shih, D. M., Tward, A. D., Lusis, A. J., Timchalk, C., Richter, R. J., Costa, L. G. and Furlong, C. E. (2005). Toxicity of chlorpyrifos and chlorpyrifos oxon in a transgenic mouse model of the human paraoxonase (PON1) Q192R polymorphism. *Pharmacogenet. Genomics* **15**, 589–598.

Crumpton, T. L., Seidler, F. J. and Slotkin, T. A. (2000). Is oxidative stress involved in the developmental neurotoxicity of chlorpyrifos? *Brain Res. Dev. Brain Res.* **121**, 189–195.

Dam, K., Seidler, F. J. and Slotkin, T. A. (1998). Developmental neurotoxicity of chlorpyrifos: Delayed targeting of DNA synthesis after repeated administration. *Brain Res. Dev. Brain Res.* **108**, 39–45.

Engel, S. M., Berkowitz, G. S., Barr, D. B., Teitelbaum, S. L., Siskind, J., Meisel, S. J., Wetmur, J. G. and Wolff, M. S. (2007). Prenatal organophosphate metabolite and organochlorine levels and performance on the Brazelton Neonatal Behavioral Assessment Scale in a multiethnic pregnancy cohort. *Am. J. Epidemiol.* **165**, 1397–1404.

Engel, S. M., Wetmur, J., Chen, J., Zhu, C., Barr, D. B., Canfield, R. L. and Wolff, M. S. (2011). Prenatal exposure to organophosphates, paraoxonase 1, and cognitive development in childhood. *Environ. Health Perspect.* **119**, 1182–1188.

Eskenazi, B., Huen, K., Marks, A., Harley, K. G., Bradman, A., Barr, D. B. and Holland, N. (2010). PON1 and neurodevelopment in children from the CHAMACOS study exposed to organophosphate pesticides in utero. *Environ. Health Perspect.* **118**, 1775–1781.

Eskenazi, B., Marks, A. R., Bradman, A., Harley, K., Barr, D. B., Johnson, C., Morga, N. and Jewell, N. P. (2007). Organophosphate pesticide exposure and neurodevelopment in young Mexican-American children. *Environ. Health Perspect.* **115**, 792–798.

Flaskos, J. (2012). The developmental neurotoxicity of organophosphorus insecticides: A direct role for the oxon metabolites. *Toxicol. Lett.* **209**, 86–93.

Furlong, C.E., Holland, N., Richter, R.J., Bradman, A., Ho, A. and

Eskenazi, B.2006) PON1 status of farmworker mothers and children as a predictor of organophosphate sensitivity. *Pharmacogenet Genomics*, **16**, 183–190.

Furlong, C. E., Richter, R. J., Seidel, S. L., Costa, L. G. and Motulsky, A. G. (1989). Spectrophotometric assays for the enzymatic hydrolysis of the active metabolites of chlorpyrifos and parathion by plasma paraoxonase/arylesterase. *Anal. Biochem.* **180**, 242–247.

Guizzetti, M., Pathak, S., Giordano, G. and Costa, L. G. (2005). Effect of organophosphorus insecticides and their metabolites on astroglial cell proliferation. *Toxicology* **215**, 182–190.

Howard, A. S., Bucelli, R., Jett, D. A., Bruun, D., Yang, D. and Lein, P. J. (2005). Chlorpyrifos exerts opposing effects on axonal and dendritic growth in primary neuronal cultures. *Toxicol. Appl. Pharmacol.* **207**, 112–124.

Irizarry, R. A., Hobbs, B., Collin, F., Beazer-Barclay, Y. D., Antonellis, K. J., Scherf, U. and Speed, T. P. (2003). Exploration, normalization, and summaries of high density oligonucleotide array probe level data. *Biostatistics* **4**, 249–264.

Langfelder, P. and Horvath, S. (2008). WGCNA: An R package for weighted correlation network analysis. *BMC Bioinformatics* **9**, 559.

Li, W. F., Costa, L. G., Richter, R. J., Hagen, T., Shih, D. M., Tward, A., Lusis, A. J. and Furlong, C. E. (2000). Catalytic efficiency determines the in-vivo efficacy of PON1 for detoxifying organophosphorus compounds. *Pharmacogenetics* **10**, 767–779.

Monnet-Tschudi, F., Zurich, M. G., Schilter, B., Costa, L. G. and Honegger, P. (2000). Maturation-dependent effects of chlorpyrifos and parathion and their oxygen analogs on acetylcholinesterase and neuronal and glial markers in aggregating brain cell cultures. *Toxicol. Appl. Pharmacol.* **165**, 175–183.

Moreira, E. G., Yu, X., Robinson, J. F., Griffith, W., Hong, S. W., Beyer, R. P., Bammler, T. K. and Faustman, E. M. (2010). Toxicogenomic profiling in maternal and fetal rodent brains following gestational exposure to chlorpyrifos. *Toxicol. Appl. Pharmacol.* **245**, 310–325.

Olmos, C., Sandoval, R., Rozas, C., Navarro, S., Wyneken, U., Zeise, M., Morales, B. and Pancetti, F. (2009). Effect of short-term exposure to dichlorvos on synaptic plasticity of rat hippocampal slices: Involvement of acylpeptide hydrolase and alpha(7) nicotinic receptors. *Toxicol. Appl. Pharmacol.* **238**, 37–46.

Qiao, D., Seidler, F. J. and Slotkin, T. A. (2001). Developmental neurotoxicity of chlorpyrifos modeled in vitro: Comparative effects of metabolites and other cholinesterase inhibitors on DNA synthesis in PC12 and C6 cells. *Environ. Health Perspect.* **109**, 909–913.

Quistad, G. B., Klintenberg, R. and Casida, J. E. (2005). Blood acylpeptide hydrolase activity is a sensitive marker for exposure to some organophosphate toxicants. *Toxicol. Sci.* **86**, 291–299.

Rauh, V. A., Garfinkel, R., Perera, F. P., Andrews, H. F., Hoepner, L., Barr, D. B., Whitehead, R., Tang, D. and Whyatt, R. W. (2006). Impact of prenatal chlorpyrifos exposure on neurodevelopment in the first 3 years of life among inner-city children. *Pediatrics* **118**, e1845–e1859.

Ray, A., Liu, J., Ayoubi, P. and Pope, C. (2010). Dose-related gene expression changes in forebrain following acute, low-level chlorpyrifos exposure in neonatal rats. *Toxicol. Appl. Pharmacol.* **248**, 144–155.

Richter, R. J. and Furlong, C. E. (1999). Determination of paraoxonase (PON1) status requires more than genotyping. *Pharmacogenetics* **9**, 745–753.

Ritchie, M. E., Diyagama, D., Neilson, J., van Laar, R., Dobrovic, A., Holloway, A. and Smyth, G. K. (2006). Empirical array quality weights in the analysis of microarray data. *BMC Bioinformatics* **7**, 261.

Schuh, R. A., Lein, P. J., Beckles, R. A. and Jett, D. A. (2002). Noncholinesterase mechanisms of chlorpyrifos neurotoxicity: Altered phosphorylation of Ca2+/cAMP response element binding protein in cultured neurons. *Toxicol. Appl. Pharmacol.* **182**, 176–185.

Shih, D. M., Gu, L., Xia, Y. R., Navab, M., Li, W. F., Hama, S., Castellani, L. W., Furlong, C. E., Costa, L. G., Fogelman, A. M., *et al.* (1998). Mice lacking serum paraoxonase are susceptible to organophosphate toxicity and atherosclerosis. *Nature* **394**, 284–287.

Slotkin, T. A. and Seidler, F. J. (2007). Comparative developmental neurotoxicity of organophosphates in vivo: Transcriptional responses of pathways for brain cell development, cell signaling, cytotoxicity and neurotransmitter systems. *Brain Res. Bull.* **72**, 232–274.

Slotkin, T. and Seidler, F. (2009). Transcriptional profiles reveal similarities and differences in the effects of developmental neurotoxicants on differentiation into neurotransmitter phenotypes in PC12 cells. *Brain Res. Bull.* **78**, 211–125.

Slotkin, T. A., Seidler, F. J. and Fumagalli, F. (2008). Targeting of neurotrophic factors, their receptors, and signaling pathways in the developmental neurotoxicity of organophosphates in vivo and in vitro. *Brain Res. Bull.* **76**, 424–438.

Smyth, G. K. (2004). Linear models and empirical Bayes methods for assessing differential expression in microarray experiments. *Stat. Appl. Genet. Mol. Biol.* **3**, Article3.

Stapleton, A. R. and Chan, V. T. (2009). Subtoxic chlorpyrifos treatment resulted in differential expression of genes implicated in neurological functions and development. *Arch. Toxicol.* **83**, 319–333.

Theiler, K. (1989). *The House Mouse: Atlas of Embryonic Development*. Springer-Verlag, New York.

USEPA (2006). *Reregistration Eligibility Decision for Chlorpyrifos*. Available at: http://www.epa.gov/oppsrrd1/reregistration/REDs/chlorpyrifos_red.pdf. Accessed October 21, 2013.

Vidal, J. L. M., Gonazlez, F. J. E., Galera, M. M. and Cano, M. L. C. (1998). Diminution of chlorpyrifos and chlorpyrifos oxon in tomatoes and green beans grown in greenhouses. *J. Agric. Food Chem.* **46**, 1440–1444.

Yamin, R., Bagchi, S., Hildebrant, R., Scaloni, A., Widom, R. L. and Abraham, C. R. (2007). Acyl peptide hydrolase, a serine proteinase isolated from conditioned medium of neuroblastoma cells, degrades the amyloid-beta peptide. *J. Neurochem.* **100**, 458–467.

Young, J. G., Eskenazi, B., Gladstone, E. A., Bradman, A., Pedersen, L., Johnson, C., Barr, D. B., Furlong, C. E. and Holland, N. T. (2005). Association between in utero organophosphate pesticide exposure and abnormal reflexes in neonates. *Neurotoxicology* **26**, 199–209.

Yuknavage, K. L., Fenske, R. A., Kalman, D. A., Keifer, M. C. and Furlong, C. E. (1997). Simulated dermal contamination with capillary samples and field cholinesterase biomonitoring. *J. Toxicol. Environ. Health* **51**, 35–55.